SCIENTIFIC REPORTS

OPEN

Terrestrial water load and groundwater fluctuation in the Bengal Basin

W. G. Burgess[1], M. Shamsudduha[2], R. G. Taylor[3], A. Zahid[4], K. M. Ahmed[5], A. Mukherjee[6], D. J. Lapworth[7] & V. F. Bense[8]

Groundwater-level fluctuations represent hydraulic responses to changes in groundwater storage due to aquifer recharge and drainage as well as to changes in stress that include water mass loading and unloading above the aquifer surface. The latter 'poroelastic' response of confined aquifers is a well-established phenomenon which has been demonstrated in diverse hydrogeological environments but is frequently ignored in assessments of groundwater resources. Here we present high-frequency groundwater measurements over a twelve-month period from the tropical, fluvio-deltaic Bengal Aquifer System (BAS), the largest aquifer in south Asia. The groundwater level fluctuations are dominated by the aquifer poroelastic response to changes in terrestrial water loading by processes acting over periods ranging from hours to months; the effects of groundwater flow are subordinate. Our measurements represent the first direct, quantitative identification of loading effects on groundwater levels in the BAS. Our analysis highlights the potential limitations of hydrogeological analyses which ignore loading effects in this environment. We also demonstrate the potential for employing poroelastic responses in the BAS and across other tropical fluvio-deltaic regions as a direct, *in-situ* measure of changes in terrestrial water storage to complement analyses from the Gravity and Climate Experiment (GRACE) mission but at much higher resolution.

Regional monitoring by the Gravity and Climate Recovery Experiment (GRACE) satellite mission[1] has prompted concerns over the sustainability of deep groundwater pumping[2], including across mega-delta regions of Asia[3] where groundwater meets the needs of over 300 million people. The largest and most densely populated flood-plain region is the Bengal Basin, which is the focus of intensive water use[4], subject to substantial hydrological seasonality[5] and highly vulnerable to climate change[6]. Here, the Rivers Ganges, Brahmaputra and Meghna (GBM) have a combined annual discharge at their confluence of $1350 \, km^3$, second only to the River Amazon. The GBM floodplains present the second largest seasonal gravity anomaly observed by the GRACE satellites[5], driven by variations in terrestrial water storage (ΔTWS), the sum of changes in surface water runoff and storage, soil water and groundwater storage. The uppermost few hundred metres of the Holocene-Pleistocene GBM floodplain sediments constitute the Bengal Aquifer System[7] (BAS), the source of domestic and irrigation water to over 100 million people[8]. 'Deep groundwater' in BAS, greater than 150 m below the floodplain surface, supplies Dhaka as well as many provincial and coastal towns and rural water supply schemes[8] where it is developed as an alternative to shallow, arsenic-contaminated groundwater[9]. Human dependency on groundwater resources, exposure of groundwater to increasing climatic and anthropogenic stresses, and geogenic constraints on water quality are features of the BAS which are common to other major Asian mega-deltas[9]. The intensity of groundwater abstraction from the BAS has prompted concern[7] over its sustainability, and focussed attention on the variability of seasonal amplitudes and secular trends in TWS, and especially of groundwater as a component of TWS. Controversy over interpretations of GRACE satellite gravity data across the Bengal Basin centres on assessments of secular groundwater depletion[3, 10] which range from 1 to $4 \, km^3$/year; the disparity is partly associated with the

[1]Department of Earth Sciences, University College London, London, WC1E 6BT, UK. [2]Institute for Risk and Disaster Reduction, University College London, London, WC1E 6BT, UK. [3]Department of Geography, University College London, London, WC1E 6BT, UK. [4]Bangladesh Water Development Board, Dhaka, Bangladesh. [5]Department of Geology, Dhaka University, Dhaka, 1000, Bangladesh. [6]Department of Geology and Geophysics, Indian Institute of Technology Kharagpur, Kharagpur, West Bengal, 721302, India. [7]British Geological Survey, Wallingford, Oxfordshire, OX10 8BB, UK. [8]Department of Environmental Sciences, Wageningen University, Wageningen, The Netherlands. Correspondence and requests for materials should be addressed to W.G.B. (email: william.burgess@ucl.ac.uk)
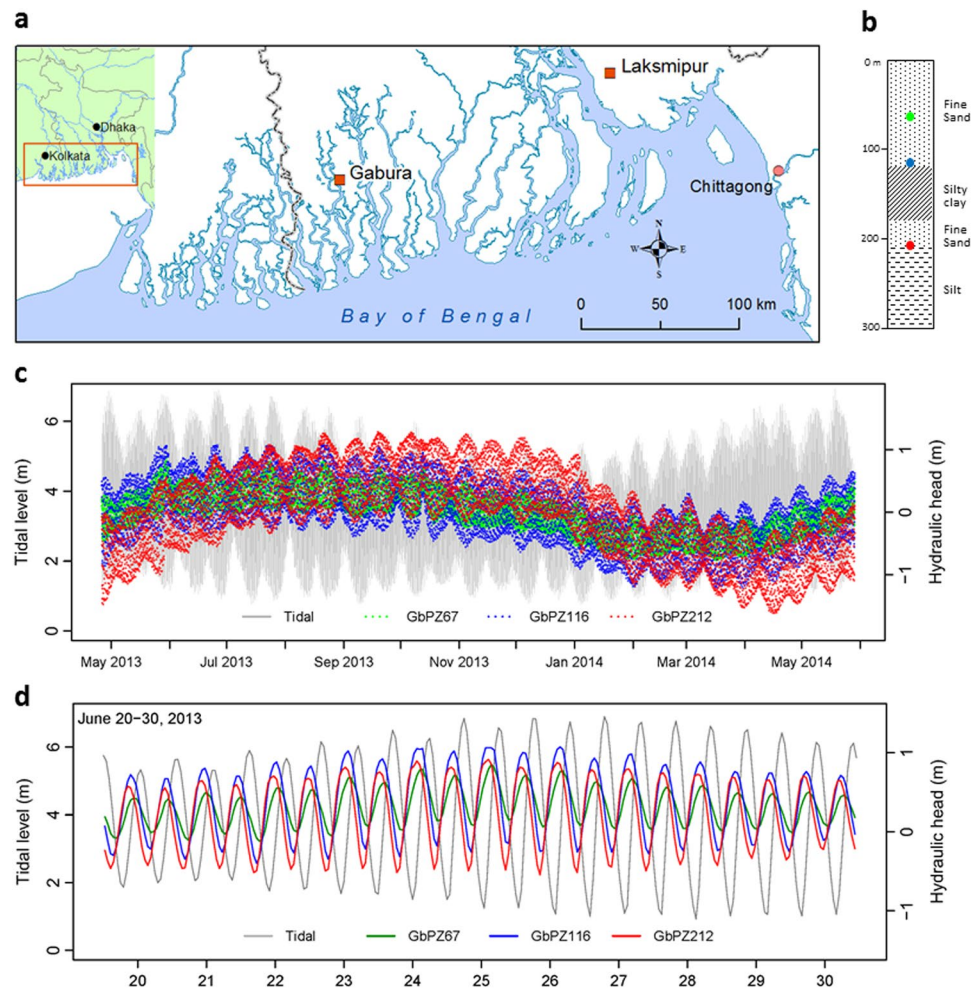
Figure 1. Study sites, hydraulic heads at Gabura and tide level at Chittagong, May 2013 to May 2014. (**a**) Location of the study sites (red squares) in southern Bangladesh (map created using ArcGIS version 10.3.1, https://www.arcgis.com/); (**b**) at Gabura, the open screen measurement points of piezometers GbPZ67 (green, depth 67 m), GbPZ116 (blue, depth 116 m), and GbPZ212 (red, depth 212 m) within the lithological profile; (**c**) the Gabura hydrographs from piezometers GbPZ67, GbPZ116, and GbPZ212 shown as equivalent fresh water head, and Chittagong tide level (grey), relative to the time series averages, May 2013 to May 2014; (**d**) the Gabura piezometer groundwater heads and the Chittagong tide, relative to the time series averages, 20th June to 30th June 2013.

choice of scaling factor applied to address amplitude damping that occurs during GRACE processing[11], and partly with the use of global hydrological models which introduce substantial uncertainty[12]. *In situ* observations offer a valuable and necessary constraint on interpretations of changes in TWS[12, 13], but despite extensive programmes of shallow water-table monitoring across the Bengal Basin[4, 14], deeper levels of BAS remain largely unmonitored[7]. Management of the deep groundwater resource in BAS, as elsewhere across south Asia, lacks a sound empirical basis.

At two sites in southern Bangladesh (Fig. 1, and Supplementary Information) we recorded absolute groundwater pressure and atmospheric pressure at hourly intervals over one year in three closely-spaced boreholes screened at depths between 65 m and 250 m. For construction and completion details of the boreholes see Methods. At Gabura the boreholes GbPZ67, GbPZ116 and GbPZ212 (the numbers indicate the depth to the top of the screen in metres) are situated a few tens of metres from a tidal channel within the GBM delta; shallow groundwater is saline[8] and groundwater pumping is insignificant. The Laksmipur boreholes LkPZ91, LkPZ152 and LkPZ244 are situated on the Lower Meghna floodplain, 10 km east of the River Meghna and 8 km from Laksmipur municipal boreholes which pump from 270–300 m depth. From the *in-situ* measurements at both sites we derived an hourly record of equivalent fresh water head at the depth of each borehole screen after correcting raw data for atmospheric pressure and salinity-density effects (see Methods). Environmental head[15] has been proposed for use when vertical groundwater flux is sought and vertical variations in groundwater density occur. Following a recent critical analysis[16], we used fresh water head to compare the temporal variation of groundwater head at specified depths in borehole water columns of constant density, where vertical flow components are not sought.
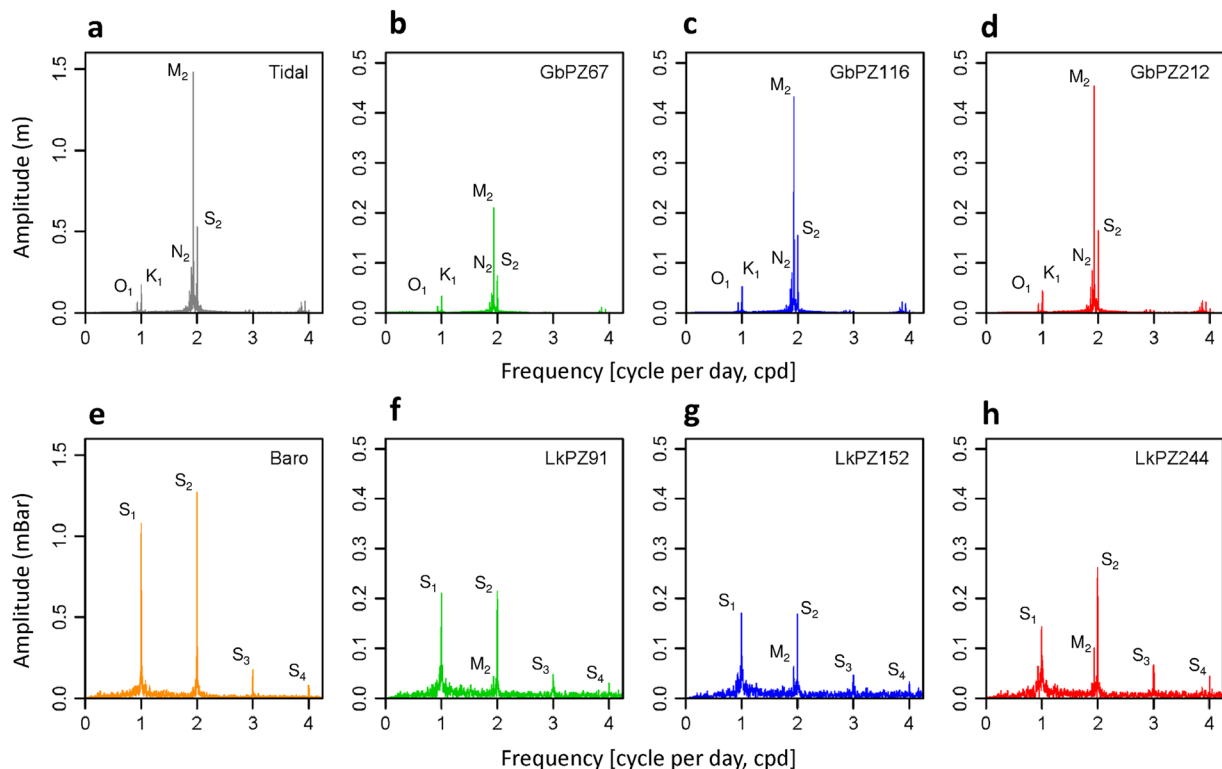
Figure 2. Amplitudes of the tidal and atmospheric signals and groundwater responses at Gabura and Laksmipur. Top: amplitude *versus* frequency for (**a**) the Chittagong tide and (**b**–**d**) the groundwater heads at GbPZ67, GbPZ116 and GbPZ212 respectively, 1st June 2013 to 31st May 2014, showing the principal solar-lunar tidal components[17] O_1, K_1, N_2, M_2 and S_2, and additional minor components (see text). Bottom: amplitude *versus* frequency for (**e**) atmospheric pressure at Laksmipur, and (**f**–**h**) groundwater pressure measured in piezometers LkPZ91, LkPZ152 and LkPZ244 respectively, over the period of hydrograph recession between 1 November 2013 and 30 April 2014.

Notation and source of tidal/atmospheric frequency components		O_1 lunar diurnal	S_1 solar diurnal	K_1 lunar-solar diurnal	N_2 lunar elliptic semi-diurnal	M_2 lunar semi-diurnal	S_2 solar semi-diurnal	S_3 solar ter-diurnal	MN_4 shallow water quarter-diurnal	M_4 shallow water overtides of principal lunar	S_4 solar quarter-diurnal
Frequency (cpd)		0.930	1.000	1.003	1.896	1.933	2.000	3.000	3.828	3.864	4.000
Tidal spectrum amplitude (m)	Chittagong tide	0.067	—	0.171	0.279	1.482	0.532	—	0.028	0.065	—
	GbPZ67	0.013	—	0.033	0.039	0.210	0.074	—	0.004	0.010	—
	GbPZ116	0.020	—	0.052	0.080	0.432	0.155	—	0.010	0.022	—
	GbPZ212	0.018	—	0.045	0.084	0.454	0.164	—	0.012	0.024	—
Atmospheric spectrum amplitude (mBar)	Atmospheric pressure	—	1.076	—	—	—	1.269	0.175	—	—	0.079
	LkPZ91	—	0.210	—	—	0.044	0.214	0.048	—	—	0.031
	LkPZ152	—	0.170	—	—	0.064	0.169	0.046	—	—	0.033
	LkPZ244	—	0.144	—	—	0.101	0.262	0.067	—	—	0.044

Table 1. Summary of the frequency components and amplitudes of the tidal and atmospheric signals and the groundwater responses at the Gabura and Laksmipur monitoring boreholes. Frequency component names follow the U.S. National Oceanic and Atmospheric Administration Tide and Current Glossary[18]. Note that the M_2 lunar semi-diurnal component in the Laksmipur (Lk) measurements is a response to earth tides.

Results

Groundwater hydrographs at a coastal site. The Gabura hydrographs (Fig. 1) demonstrate distinctive periodic oscillations containing the principal solar-lunar tidal frequencies[17] O_1, K_1, N_2, M_2 and S_2 and the minor components[18] MN_4 and M_4 (Fig. 2). The oscillations are close to synchronous at all three depths of measurement and amplitudes increase between GbPZ67 and GbPZ116; a summary of amplitudes for specific frequencies is given in Table 1. Subsurface hydraulic responses to a surface sinusoidal hydraulic impulse would dissipate exponentially with depth[19] according to T, the period of the impulse, and D, the vertical hydraulic diffusivity (vertical hydraulic conductivity, K_v, divided by specific storage, S_s) of the sediments. For the BAS, a value of $1.5 \times 10^{-4}\,\mathrm{m^2/s}$
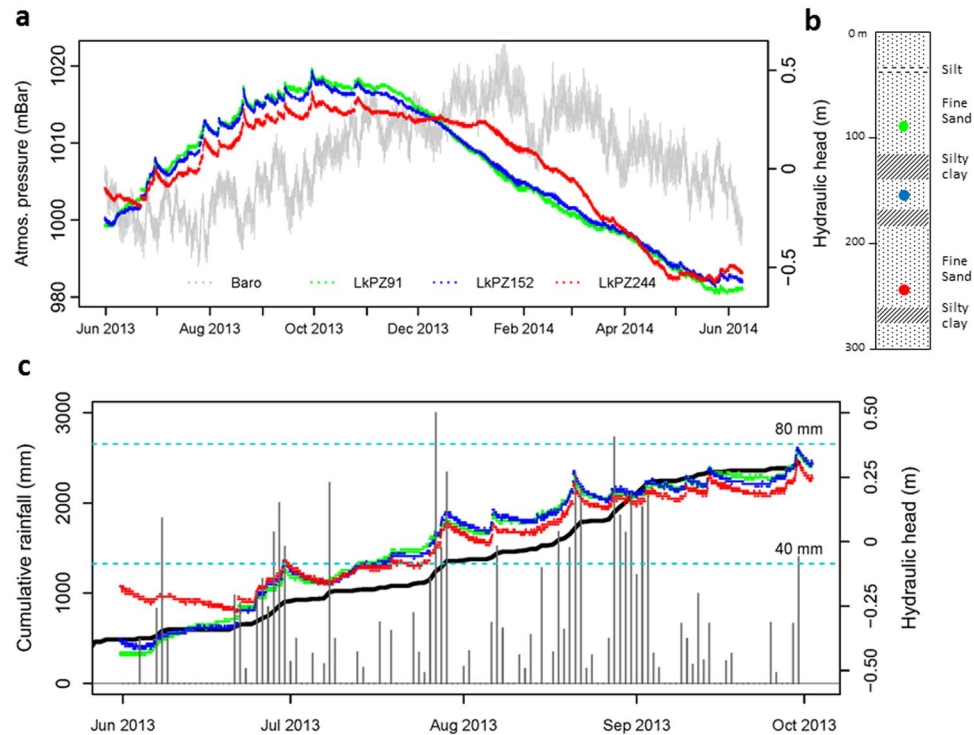
Figure 3. Hydraulic heads and rainfall at Laksmipur, June 2013 to June 2014. (**a**) The Laksmipur hydrographs at piezometers LkPZ91 (green, depth 91 m), LkPZ152 (blue, depth 152 m), LkPZ244 (red, depth 244 m) shown as equivalent fresh water head relative to the time series averages, and contemporaneous atmospheric pressure measured at the site; (**b**) the open screen measurement points of piezometers LkPZ91 (green), LkPZ152 (blue), and LkPZ244 (red) within the lithological profile; (**c**) daily rainfall (vertical bars, scale given as horizontal blue dashed lines) and cumulative rainfall (black line) superimposed on the hydraulic heads of LkPZ91, LkPZ152 and LkPZ244 as in (**a**). Note that the daily rainfall measurements are from a rain gauge 7 km distant from the Laksmipur multi-level piezometer site (Supplementary Information).

for D derived from K_v and S_s determined by inverse modelling[20], suggests that hydraulic penetration of the diurnal tidal signal would be less than 10 m; the spring-neap tidal signal should not penetrate beyond a few tens of metres. Therefore we interpret the undamped periodic oscillations at up to 212 m depth as the fluid pressure changes in this coastal, confined and unconsolidated aquifer due to mechanical loading and unloading of the aquifer by tidal water movements above the aquifer surface, commensurate with analytical treatments[21–23].

Groundwater hydrographs at an inland site. At Laksmipur (Fig. 3), tidal water loading influences are absent; the hydrographs are characterised by a sequence of episodic increments superimposed on a rising trend throughout the monsoon season. Periodic components are minor compared to Gabura and are dominated by responses to the atmospheric frequency signals S_1 and S_2 (Fig. 2), of which only the diurnal component S_1 shows a consistent trend with depth. During undisturbed periods of dry-season recession, a clear inverse relationship between atmospheric pressure and groundwater pressure is revealed (Fig. 4). As at Gabura, groundwater head variations at Laksmipur are close to simultaneous, within a 2–3 hour time period, and of similar magnitude at the three depths of measurement. Whereas a surface hydraulic impulse undergoes delay and dissipation with depth dependent on the sediment hydraulic diffusivity[24], neither are evident in the Laksmipur hydrographs. Therefore the episodic increments cannot be explained as the hydraulic consequence of groundwater storage replenishment. Nevertheless the increments are closely associated in time with periods of heavy rainfall (Fig. 3c), measured at a gauge 7 km distant from the piezometer site (Supplementary Information). We interpret the increments in groundwater head at LkPZ91, LkPZ152 and LkPZ244, by analogy with the tidal loading situation at Gabura, as the almost instantaneous hydraulic consequence of the aquifer poroelastic response to terrestrial water loading associated with episodic monsoonal saturation and flooding of the land surface. The rising groundwater heads also track cumulative rainfall (Fig. 3c), which acts as a proxy for surface water loading. Therefore we interpret the coherent seasonal trend recorded between 91 and 244 m depth at Laksmipur as the fluid pressure response to mechanical loading above the aquifer surface through accumulation of terrestrial water as the monsoon progresses. By inverse analogy with the Laksmipur hydrograph rising limbs, we interpret the extended groundwater head recessions principally as the response to unloading of the land surface through a combination of river flood recession, surface water drainage, shallow groundwater drainage and evapotranspiration. The influence of deep groundwater flow may be present in the delay to the start of recession at LkPZ244, the deepest Laksmipur piezometer, relative to LkPZ91 and LkPZ152 (Fig. 3a), but in general it is subordinate to the hydro-mechanical response over the time period of the data record. We note the similarity in the magnitude of annual fluctuation in
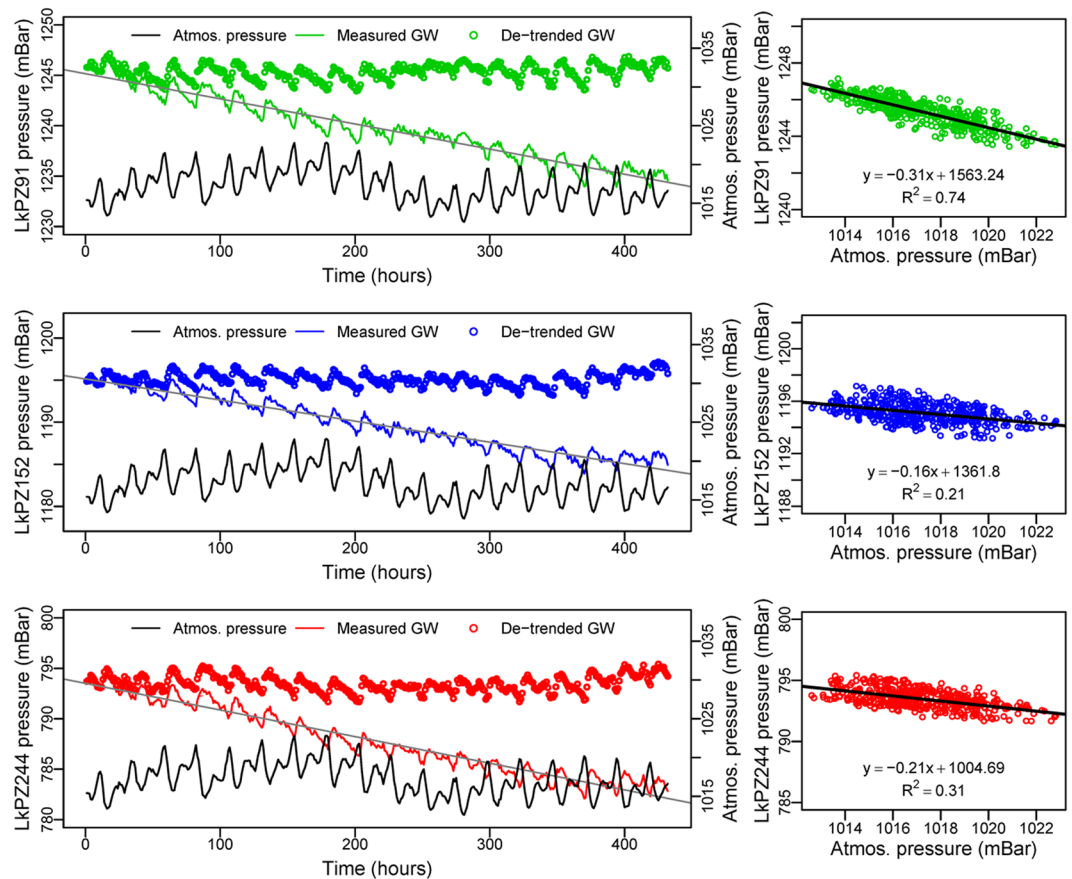
Figure 4. Barometric efficiency, *B*, determined from the inverse relationship between atmospheric pressure and groundwater pressure. Left: Atmospheric pressure (black line) and measured groundwater (GW) pressure at LkPZ91 (green line), LkPZ152 (blue line) and LkPZ244 (red line) with the linear recession trends (grey lines) and as de-trended groundwater pressure series (open circles, colours as above); time is in hours, from 00.00 hours on 14/1/2014 to 24.00 hours on 31/1/2014. Right: De-trended groundwater pressure at LkPZ91 (green), LkPZ152 (blue) and LkPZ244 (red) versus atmospheric pressure, giving the barometric efficiency, B, as the negative value of the linear regression slope.

head (of order 1 m) at LkPZ244 with that at GbPZ212, the deepest point of measurement at Gabura, and suggest this is due to a similar monsoonal water loading experienced at the two locations.

Discussion

Poroelastic effects in the Bengal Aquifer System. At both the coastal and the inland sites, over the annual duration of measurements, the data indicate groundwater heads responding dominantly to mechanical loading and unloading due to changes in terrestrial water storage above the aquifer surface by tidal and hydrological processes acting over periods ranging from hours to months and determined by poroelasticity; the effects of groundwater flow are subordinate. Poroelastic responses in the BAS have indeed been predicted[25]. They are favoured by the low topographic relief which restricts gravitational groundwater flow[26], the low vertical hydraulic conductivity which further constrains depth of groundwater circulation[20, 27], and the pronounced sediment compressibility[5] reflected in high S_s. Heavy monsoon rainfall and deep surface water flooding[10] provide a large water load. Hydraulic diffusivity, *D*, controls the relative importance of poroelastic effects as compared to transient groundwater flow on the hydraulic heads of an aquifer. The vertical hydraulic diffusivity of BAS is low because the many silt-clay layers distributed throughout the fluvio-deltaic sediments[20, 27] impose a low value of K_v, and the sediment compressibility, hence S_s, is high[5].

We focus on the short-term groundwater pressure transients up to annual time periods because these are the transients that are definitive of the poroelastic response. Projection of secular trends requires a multi-year record, therefore no assessment of potentially longer-term trends linked to groundwater abstraction has been made. The hydrographs have likely not captured the start of the 2013 monsoon season, so any assessment of longer-term trends might be highly misleading. From the strong groundwater pressure responses to mechanical loading, associated poroelastic deformation of the aquifer would be expected, the nature and scale of deformation depending on the drainage condition[28]. No actual measurements of aquifer deformation are available for BAS, although a clear seasonal deflection of the ground surface across Bangladesh with an amplitude of approximately 0.06 m has been observed and associated with larger-scale, deep crustal deformation by monsoon water loading across the entire Bengal Basin[5].

Fourier analysis[17, 29] of the time series of tidal and atmospheric signals and groundwater heads provides detail of the periodic loads on the BAS (Fig. 2, Table 1). At Gabura, groundwater responses to the solar-lunar tidal components are undamped and in-phase to the depth of GbPZ212, critical evidence for the dominantly mechanical response of the aquifer at these depths to periodic tidal loading at the surface. At Laksmipur, groundwater responses to the diurnal and semi-diurnal atmospheric frequencies are likewise largely undamped to the depth of LkPZ244; they enable a direct evaluation of barometric efficiency from the relative amplitudes of the atmospheric signals and their groundwater responses. At Laksmipur the main lunar semi-diurnal (M_2) component of the earth tide is also evident, at an increasing amplitude with depth, while at Gabura any earth tide response is masked by the dominant tidal load responses at the frequencies common[17] to all ocean and earth tides.

Implications for groundwater resources. Under the conditions found at Gabura and Laksmipur, the conventional principle of groundwater resource monitoring, which assumes negligible loading influence, is invalid. Borehole water levels do not fluctuate solely, or principally, on account of changes in groundwater storage: rising water levels in deep monitoring boreholes do not necessarily indicate replenishment and falling water levels may not imply depletion of groundwater storage. On the contrary, groundwater heads at over 200 m depth at one coastal location and one inland location (Gabura and Laksmipur respectively) respond rapidly, within a few hours, to distinctive loading signals, consistent with poroelastic[28] deformation being the dominant process controlling the observed changes in hydraulic head. We have made similar observations[30] at six additional sites between West Bengal, India, and eastern Bangladesh; the phenomenon may therefore be widespread throughout the Bengal Basin. Additional observations are necessary to confirm the scale of the poroelastic responses in the variety of geomorphological and hydrological contexts of the Basin, but it is likely that assessments of groundwater recharge[31] and groundwater storage changes[10, 32] across the Basin, based solely on hydraulic analyses of groundwater hydrographs, need to be revisited. Uncoupled, solely hydraulic treatments of transient groundwater conditions which ignore the possibility of loading effects, including the calibration of transient groundwater flow models[33] using groundwater hydrographs, must likewise be in doubt.

Geological weighing lysimetry in the Bengal Basin. Observations of groundwater levels responding to changes in near-surface water mass, equivalent to those reported here, have been made in diverse geological and hydrological environments worldwide and underlie the concept of 'geological weighing lysimeters'[34–39]. The approach employs the equation governing one-dimensional, transient groundwater pressure $\left(\frac{\partial p}{\partial t}\right)$ in permeable, elastically compressible sediments under purely vertical strain[35]:

$$\frac{\partial p}{\partial t} = D\frac{\partial^2 p}{\partial z^2} + C\frac{\partial \sigma_T}{\partial t} \qquad (1)$$

where the first term on the right describes flow-induced changes, and the second term describes the effect of changes in vertical stress, or mass loading. D is the sediment hydraulic diffusivity (hydraulic conductivity divided by specific storage); C is the sediment loading efficiency (dimensionless), which has a value between 0 and 1 according to the distribution of surface load between the confined water and the solid matrix; and σ_T is the total vertical stress applied as a mechanical load on the formation. Conventional hydrogeological analysis neglects the second term on the right of Eq. (1), effectively uncoupling the flow field from the stress field on the premise that poroelastic effects are normally secondary to hydraulic effects. Where groundwater flow is negligible, however, groundwater pressure responds instantaneously to addition or subtraction of mechanical load[19], as governed by:

$$\frac{\partial p}{\partial t} = C\frac{\partial \sigma_T}{\partial t} \qquad (2)$$

Groundwater head response to tidal loading at Gabura potentially provides an empirical means for a direct measure of loading efficiency C, the proportional change in groundwater pressure relative to change in total vertical stress, and hence the possibility of applying geological weighing lysimetry in the Bengal Basin. However the actual tidal signal at Gabura, where the coastline is densely dissected by tidal channels, is unknown and likely considerably different to the Chittagong tide. Therefore we determined C indirectly through its relationship[21] with barometric efficiency, B, where:

$$B + C = 1 \qquad (3)$$

Determination of B requires that influences on groundwater head other than atmospheric pressure can be estimated and subtracted from the measurements, or are minor in comparison to the atmospheric effects, or are absent[17]. At Gabura, barometric effects are obscured by the tidal responses which are more than two orders of magnitude greater than the atmospheric signal (Fig. 2). However at Laksmipur, during undisturbed periods of dry-season recession (Fig. 3), the trend of groundwater head decline can be determined and subtracted to reveal the inverse relationship between atmospheric pressure and groundwater pressure (Fig. 4). Barometric efficiency determined by linear regression of this relationship[17] is 0.31 ± 0.02 (LkPZ91), 0.16 ± 0.03 (LkPZ152) and 0.21 ± 0.03 (LkPZ244), giving values for loading efficiency, C, from Eq. (3) as 0.69 ± 0.02 (LkPZ91), 0.84 ± 0.03 (LkPZ152) and 0.79 ± 0.03 (LkPZ244); ranges are $\pm$ twice the standard error in each case (Table 2). The mean value of C by this method is 0.77. The Fourier method[17, 29] applied to the solar diurnal, S_1, and semi-diurnal, S_2, atmospheric frequency components and groundwater responses (Fig. 2, Table 1) indicates values for B of 0.19-0.16 (LkPZ91), 0.16-0.13 (LkPZ152) and 0.13-0.21 (LkPZ244). The mean values for loading efficiency, C, from Eq. (3) by the Fourier method are 0.82 (LkPZ91), 0.85 (LkPZ152) and 0.83 (LkPZ244). The two approaches illustrate the variability in C for BAS and yield values consistent with measurements of loading efficiency at geological

	Loading efficiency C		Maximum fresh water head (m)	Minimum fresh water head (m)	Accumulated fresh water head (m)	Accumulated head (m), corrected for B	Accumulated TWS (m)	
	(regression)	(Fourier, S1–S2)					(C_r)	(C_F)
LkPZ91	0.69 ± 0.02	0.81–0.84	6.78	5.98	0.80	0.80	1.15	0.97
LkPZ152	0.84 ± 0.03	0.84–0.87	7.69	6.91	0.78	0.77	0.92	0.91
LkPZ244	0.79 ± 0.03	0.87–0.79	3.69	3.11	0.58	0.59	0.74	0.71

Table 2. Monsoon seasonal TWS accumulation over the Laksmipur piezometer sensing areas. Ranges of values for loading efficiency, C, by regression analysis are ± twice the standard error; ranges of C by Fourier analysis are by reference to the S_1 and S_2 atmospheric frequency components determined independently. C_r denotes application of C as determined by regression; C_F denotes application of C as determined by Fourier.

weighing lysimeter sites elsewhere[34, 36, 37] but uncertainty remains in the evaluated range between 0.67 and 0.87. There is no consistent trend with depth.

Applying the Laksmipur boreholes as geological weighing lysimeters[34] (see Methods) we evaluated seasonal inundation over the 2013 monsoon period, ΔTWS_m (Table 2). In an infinite, uniform half-space, 90% of the terrestrial water loading signal derives from a 'sensing area' of radius approximately ten times the borehole depth[35], *i.e.* 3 km² (LkPZ91), 10 km² (LkPZ152) and 20 km² (LkPZ244). We determined ΔTWS_m directly from the accumulation of groundwater head (as equivalent fresh water head) recorded between the start (h_1) and end (h_2) of the rising limbs of the groundwater hydrographs and accounting for loading efficiency, C, where:

$$\Delta TWS_m = (h_2–h_1)/C \qquad (4)$$

By this analysis, using the estimates of C from evaluation of B by linear regression and Fourier analysis, seasonal inundation during the 2013 monsoon period averaged 0.90 m effective water depth, ranging from 1.15 m (LkPZ91) to 0.71 m (LkPZ244) and possibly underestimating the full seasonal inundation if, as noted, the hydrographs have not captured the start of the monsoon. As the integrated seasonal accumulation of water mass, ΔTWS_m is the same variable as measured by GRACE at a scale[1] of approximately 10⁵ km², assessments of which range from 0.49 to 0.75 m per monsoon season across the GBM floodplains over the period 2003–2007[5, 10] and 0.51 m for 2013 (Supplementary Information). Differences potentially arising from the large contrast in observation scale highlight possible within-basin variability of ΔTWS. Discrepancy may additionally be due to amplitude damping that occurs during GRACE processing[11], for which no ground-truth basis for a scaling correction currently exists.

Modelling investigation of depth and extent of the loading influences.

To further explore the hydro-mechanical BAS response to ΔTWS, we assembled characteristics of the aquifer in a numerical model of coupled vertical strain and groundwater flow in one-dimension (see Methods). A value of $C = 0.75$ was chosen as representative for the BAS, approximately central to the range of determined values. The significance of uncertainty in C was explored by applying the minimum ($C = 0.67$) and maximum ($C = 0.87$) values of the determined range. The simulations reproduce the characteristic features of the Gabura and Laksmipur hydrographs (Fig. 5, and Supplementary Information). Results are consistent with conclusions of hydrograph analysis that the deep groundwater head variations monitored over a twelve month period are inexplicable without reference to poroelasticity. The purely hydraulic response, when $C = 0$ (Fig. 5b and e), is significantly overprinted by poroelastic effects at all values of C within the determined range when vertical hydraulic diffusivity values representative of BAS are applied (Fig. 5c and f, and Supplementary Information). The modelled hydrograph peaks are synchronous with the surface water loading signal, and the poroelastic effect becomes increasingly dominant with depth (Fig. 5d and g). In the tidal scenario, the shorter period of the spring/neap tidal signal compared to monsoonal forcing leads to shallower penetration of the hydraulic response, so the poroelastic influence is more uniformly dominant throughout the stratigraphic column. Modelling therefore confirms that ignoring poroelastic effects on hydraulic head would lead to false conclusions in respect of aquifer replenishment and depletion.

The depth at which poroelastic effects become important can vary greatly from one location to another, depending largely on the permeability structure of the overlying formations. Poroelastic dominance has been recorded at 40 m (New Zealand[34]) and 52 m (South Carolina, USA[36]). The model results (Fig. 5 and Supplementary Information) suggest that poroelastic effects in BAS may become significant at depths much shallower than reported here for Gabura and Laksmipur. In the monsoon scenarios with $C = 0.75$, poroelasticity imposes a relative difference exceeding 25% of the purely hydraulic response at depths as shallow as 25 m (Fig. 5d), thus affecting water levels over approximately half the hydrological year including the monsoon season (when groundwater levels are higher than otherwise) and the dry season (when groundwater levels are lower than otherwise). Boreholes used for groundwater level monitoring by the Bangladesh Water Development Board range from less than 5 m to 77 m depth (median 30 m, n = 1035)[4]; 76% (n = 790) are deeper than 25 m and are therefore vulnerable to significant poroelastic disturbance where confined conditions pertain.

Conclusions

Our findings expose the magnitude of the poroelastic effects of terrestrial water loading on the largest fluvio-deltaic aquifer system in south Asia. They challenge the validity of the traditional philosophy of borehole water level measurement as a means to monitor groundwater storage and recharge in BAS[10, 31, 32] and possibly
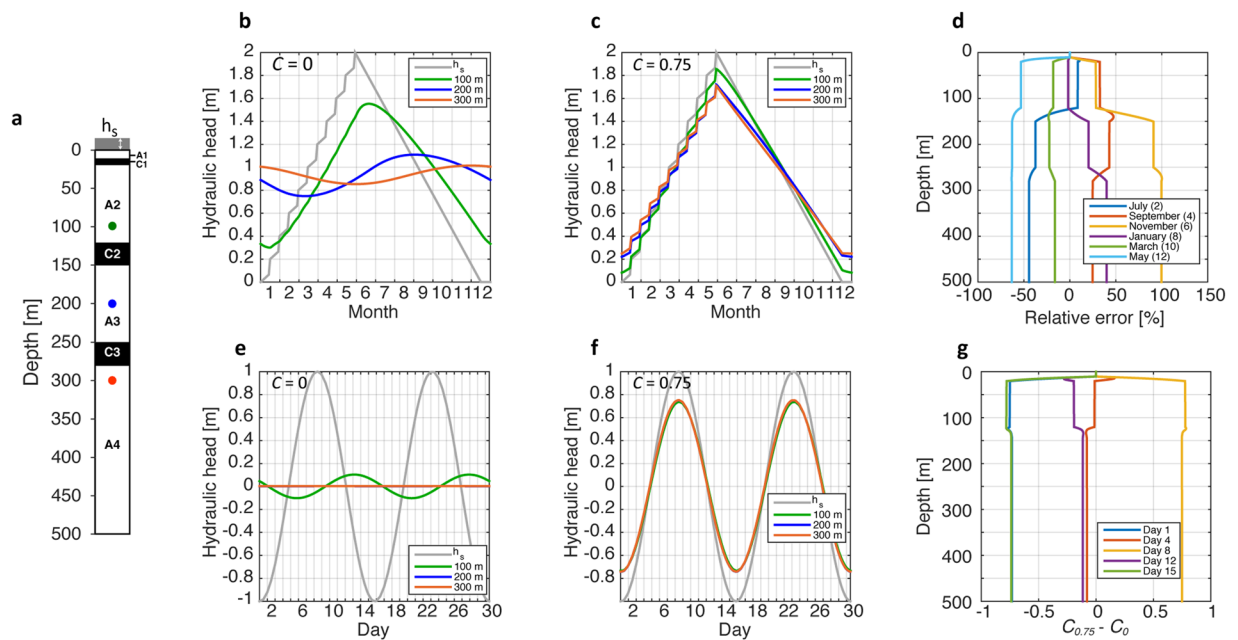
Figure 5. Model simulations showing the influences of poroelasticity. (**a**) Model configuration of permeable (A1-4) and confining (C1-3) units, with parameter values (A1-4) $K = 10^{-5}$ m/s, $S_s = 10^{-5}$ m^{-1}; (C1-3) $K = 10^{-8}$ m/s, $S_s = 10^{-4}$ m^{-1}. A column of fresh water at the surface (h_s) represents surface water depth. Colour-coded dots at depths 100 m (green), 200 m (blue) and 300 m (red) show where hydraulic head is reported for a monsoonal (**b** and **c**) and a tidal (**e** and **f**) scenario for different values of C. A value for $C = 0.75$ was chosen as representative for the BAS, as described in the text. In (**d**) the relative difference between the monsoonal scenario simulations with $C = 0$ and $C = 0.75$ is expressed as relative error calculated as $\frac{C_{0.75} - C_0}{C_0}$; in (g) the absolute difference between the tidal scenario simulations with $C = 0$ and $C = 0.75$ is illustrated.

	Gabura			Laksmipur		
	GbPZ67	GbPZ116	GbPZ212	LkPZ91	LkPZ152	LkPZ244
Depth (m, below ground level)	67	116	212	91	152	244
Electrical conductivity (μS/cm)	8150	9410	3270	19460	18300	539
Temperature (°C)	27.4	28.0	29.0	27.2	26.9	28.7
Density (kg/m³)	1000	1001	998	1006	1005	996

Table 3. Screen depths and groundwater electrical conductivity, temperature, and density for the boreholes at Gabura and Laksmipur, southern Bangladesh; borehole names include numbers which indicate the screen depth in metres, at which the head determinations apply.

other extensive fluvio-deltaic aquifers of the Asian mega-deltas. More generally, they challenge the application of uncoupled, solely hydraulic treatments of transient groundwater conditions in these regions[33]. Strategies for management and monitoring of groundwater resources in the fluvio-deltaic aquifers of south Asia should consider a broader, coupled hydro-mechanical approach which acknowledges poroelasticity.

Applying determinations of loading efficiency at Laksmipur, we have made the first direct, *in-situ* determination of ∆TWS in a tropical fluvio-deltaic environment. Results complement GRACE determinations made across much larger spatial scales and at lower temporal resolution. We propose that multiple nests of deep boreholes across the GBM floodplains could be used to establish the scale of within-basin variability of ∆TWS and to allow a direct calibration[25] of the magnitude of scaling factors applied in GRACE assessments.

Methods

Determination of equivalent fresh water head. We recorded absolute groundwater pressure in three boreholes at each of two sites in southern Bangladesh (Table 3) using 'In-Situ Rugged Troll 100' piezoresistors suspended at a known depth approximately 10 m below the static water level and set to record at hourly intervals. The boreholes were drilled by direct-circulation rotary drilling, and completed with PVC casing and a 10 m length of screen at the base, the annular space between casing and borehole wall being sealed with a bentonite and clay mixture to ensure isolation of the head measurement interval. We installed a barometric recorder in the air-filled section of one piezometer at each site to record atmospheric pressure. We evaluated groundwater density at each

piezometer from electrical conductivity, a proxy for total dissolved solid content, and temperature measured in the discharge line of a submersible pump. Three well volumes were flushed prior to making measurements. We took the ratio of dissolved solids concentration in mg/L to electrical conductivity in μS/cm as 0.65 and determined density as function of temperature and concentration following standard relationships[40].

To determine equivalent fresh water head at each piezometer screen, first we subtracted barometric pressure from *in-situ* measurements of absolute groundwater pressure to obtain gauge pressure, p_w. Then we computed equivalent fresh water head, h_f (m, relative to local datum), taking account of the piezoresistor depth and the groundwater density:

$$h_f = (e - z_1) + (p_w + p_t)/(1000^*g) \tag{5}$$

$$p_t = (z_1 - z_2)\rho_f \cdot g \tag{6}$$

where:
  e is elevation of the piezometer reference measurement point relative to local datum (m);
  z_1 is depth of the piezometer open section, below the piezometer reference point (m);
  p_w is gauge pressure at the piezoresistor (Pa);
  p_t is pressure at the piezometer screen due to fluid below the piezoresistor (Pa);
  z_2 is depth of the piezoresistor, below the piezometer reference point (m);
  ρ_f is groundwater density (kg/m^3);
  g is acceleration due to gravity.

Frequency analysis of the periodic loading signals and groundwater responses.
Frequency analysis of the atmospheric, tidal and groundwater time series was implemented using the Fast Fourier Transform (FFT) algorithm in the R programming language[41] (version 3.0.1). FFT was performed after the hourly time series data were detrended using a 25-point (i.e. 25-hour) moving average in order to remove the lower frequency components.

Evaluating monsoon season accumulation of terrestrial water storage (TWS$_m$).
Monsoon seasonal TWS accumulation was determined (Table 2) for the sensing area of each piezometer at the Laksmipur site from the difference in the equivalent fresh water head calculated at the time of maximum head, at 5.00 am on 30/9/2013 in all cases, and the minimum head at the onset of the monsoon evident at 11.00 am 4/6/2013 (LkPZ91), midday 4/6/2013 (LkPZ152), and midday 20/6/2013 (LkPZ244), using Eq. (4) after correction for barometric effects. Acknowledging uncertainty in the value of loading efficiency, C, the range of values obtained from evaluation of barometric efficiency, B, by linear regression and Fourier analysis was applied.

Modelling coupled vertical strain and groundwater flow.
We applied a numerical model to simulate the combined poroelastic and hydraulic response of the BAS aquifer using a generalised layered representation of the BAS hydrostratigraphy (Fig. 5) and an equivalent uniform representation (Supplementary Information). We used the generic finite-element code FlexPDE (pdesolutions.com) for this purpose, which has been tested in earlier modelling studies to simulate poroelastic effects[42]. Models were one-dimensional and solve a hydraulic head based version of Eq. (1). Values of vertical hydraulic conductivity, K_v, and specific storage, S_s, are consistent with the uniform BAS aquifer representation in a basin-scale numerical model[20]. A single value of loading efficiency, C, is applied (Fig. 5), making the model results indicative rather than representative of a specific site. The full range of determined values of C, including uncertainty, was applied in successive runs of the uniform aquifer representation (Supplementary Information). As a surface boundary condition, the hydraulic head is varied in accordance with an idealized monsoonal or spring/neap tidal loading scenario representing the changing depth of water at the surface. At the base the of the model domain no fluid flow is allowed. Models were run for a time-period of ten years at which point a dynamic steady state is reached and results were analysed.

Data Availability.
The datasets both generated and analysed during the current study are available from the corresponding author on reasonable request.

References
1. Tapley, B. D., Bettadpur, S., Ries, J. C., Thompson, P. F. & Watkins, M. M. GRACE measurements of mass variability in the Earth system. *Science* **305**, 503–505 (2004).
2. Wada, Y. *et al.* Global depletion of groundwater resources. *Geophys. Res. Lett.* **37**, L20402, doi:10.1029/2010GL044571 (2010).
3. Tiwari, V. M., Wahr, J. & Swenson, S. Dwindling groundwater resources in northern India, from satellite gravity observations. *Geophys. Res. Lett.* **36**, L18401, doi:10.1029/2009GL039401 (2009).
4. Shamsudduha, M., Chandler, R. E., Taylor, R. G. & Ahmed, K. M. Recent trends in groundwater levels in a highly seasonal hydrological system: the Ganges-Brahmaputra-Meghna Delta. *Hydrol. Earth Syst. Sci.* **13**, 2373–2385, doi:10.5194/hess-13-2373-2009 (2009).
5. Steckler, M. S. *et al.* Modeling earth deformation from monsoonal flooding in Bangladesh using hydrographic, GPS and GRACE Data. *J. Geophys. Res.* **115**, B08407, doi:10.1029/2009JB007018 (2010).
6. Haddeland, I. *et al.* Global water resources affected by human interventions and climate change. *Proc. Nat. Acad. Sci* **111**, 3251–3256 (2014).
7. Burgess, W. G. *et al.* Vulnerability of deep groundwater in the Bengal Aquifer System to contamination by arsenic. *Nature Geoscience* **3**, 83–87, doi:10.1038/ngeo750 (2010).
8. Ravenscroft, P. In *Groundwater resources and development in Bangladesh - background to the arsenic crisis, agricultural potential and the environment* (eds A. A. Rahman & P. Ravenscroft) Ch. 3, 43–86 (Bangladesh Centre for Advanced Studies, University Press Ltd., 2003).

9. Fendorf, S., Michael, H. A. & van Geen, A. Spatial and temporal variations of groundwater arsenic in south and southeast Asia. *Science* **328**, 1123–1127 (2010).
10. Shamsudduha, M., Taylor, R. G. & Longuevergne, L. Monitoring groundwater storage changes in the highly seasonal humid tropics: validation of GRACE measurements in the Bengal Basin. *Water Resour. Res.*, W02508, doi:10.1029/2011WR010993 (2012).
11. Swenson, S. C. & Wahr, J. Multi-sensor analysis of water storage variations of the Caspian Sea. *Geophysical Research Letters* **34**, doi:10.1029/2007GL030733 (2007).
12. Alley, W. M. & Konikow, L. F. Bringing GRACE down to Earth. *Groundwater Published online 5 Oct 2015*, doi:10.1111/gwat.12379 (2015).
13. MacDonald, A. M. *et al.* Groundwater quality and depletion in the Indo-Gangetic Basin mapped from *in situ* observations. *Nature Geoscience* **9**, 762–766, doi:10.1038/ngeo2791 (2016).
14. Bonsor, H. C. *et al.* Hydrogeological typologies of the Indo-Gangetic basin alluvial aquifer, South Asia. *Hydrogeology Journal*, doi:10.1007/s10040-017-1550-z (2017).
15. Lusczynski, N. J. Head and flow of ground water of variable density. *Journal of Geophysical Research* **66**, 4247–4256 (1961).
16. Post, V., Kooi, H. & Simmons, C. Using hydraulic head measurements in variable-density ground water flow analyses. *Ground Water* **45**, 664–671 (2007).
17. Merritt, M. L. Estimating hydraulic properties of the Floridan Aquifer System by analysis of earth-tide, ocean-tide and barometric effects, Collier and Hendry Counties, Florida. *U. S. Geological Survey Water Resources Investigation Report* 03–4267, 70 pp (2004).
18. Hicks, S. D. *et al. Tide and Current Glossary.* (US National Oceanic and Atmospheric Administration, 2000).
19. van der Kamp, G. & Maathuis, H. Annual fluctuations of groundwater levels as a result of loading by surface moisture. *Journal of Hydrology* **127**, 137–152 (1991).
20. Michael, H. & Voss, C. Estimation of regional-scale groundwater flow properties in the Bengal Basin of India and Bangladesh. *Hydrogeology Journal* **17**, 1329–1346, doi:10.1007/s10040-009-0443-1 (2009).
21. Jacob, C. E. On the flow of water in an elastic artesian aquifer. *Transactions of the American Geophysical Union*, 574–586 (1940).
22. van der Kamp, G. Tidal fluctuations in a confined aquifer extending under the sea. *International Geological Congress* **24**, 101–106 (1972).
23. Boutt, D. F. Poroelastic loading of an aquifer due to upstream dam releases. *Ground Water* **48**, 580–592 (2010).
24. Keller, C. K., van der Kamp, G. & Cherry, J. A. A multiscale study of permeability of a thick clayey till. *Water Resources Research* **25**, 2299–2317 (1989).
25. Bardsley, W. E. & Campbell, D. J. Natural geological weighing lysimeters: calibration tools for satellite and ground surface gravity monitoring of subsurface water-mass change. *Natural Resources Research* **9**, 147–156 (2000).
26. Ravenscroft, P., Burgess, W. G., Ahmed, K. M., Burren, M. & Perrin, J. Arsenic in groundwater of the Bengal Basin, Bangladesh: Distribution, field relations, and hydrogeological setting. *Hydrogeology Journal* **13**, 727–751, doi:10.1007/s10040-003-0314-0 (2005).
27. Hoque, M. A., Burgess, W. G. & Ahmed, K. M. Integration of aquifer geology, groundwater flow and arsenic distribution in deltaic aquifers - A unifying concept. *Hydrological Processes*, doi:10.1002/hyp.11181 (2017).
28. Neuzil, C. E. Hydromechanical coupling in geological processes. *Hydrogeology Journal* **11**, 41–83 (2003).
29. Acworth, R. I., Rau, G. C., McCallum, A. M., Andersen, M. S. & Cuthbert, M. O. Understanding connected surface-water/ groundwater systems using Fourier analysis of daily and sub-daily head fluctuations. *Hydrogeology Journal* **23**, 143–159, doi:10.1007/s10040-014-1182-5 (2015).
30. MacDonald, A. M. *et al.* Groundwater Resources in the Indo-Gangetic Basin: resilience to climate change and abstraction, British Geological Survey Open Report OR/15/047. 63 pp. (British Geological Survey, Nottingham, UK, 2015).
31. Shamsudduha, M., Taylor, R. G., Ahmed, K. M. & Zahid, A. The impact of intensive groundwater abstraction on recharge to a shallow regional aquifer system: evidence from Bangladesh. *Hydrogeology Journal* **19**, 901–916, doi:10.1007/s10040-011-0723-4 (2011).
32. Asoka, A., Gleeson, T., Wada, Y. & Mishra, V. Relative contribution of monsoon precipitation and pumping to changes in groundwater storage in India. *Nature Geoscience*. doi:10.1038/NGEO2869 (2017).
33. Michael, H. & Voss, C. Controls on groundwater flow in the Bengal Basin of India and Bangladesh: regional modeling analysis. *Hydrogeology Journal* **17**, 1561–1577, doi:10.1007/s10040-008-0429-4 (2009).
34. Bardsley, W. E. & Campbell, D. J. A new method for measuring near-surface moisture budgets in hydrological systems. *Journal of Hydrology* **154**, 245–254 (1994).
35. van der Kamp, G. & Schmidt, R. Monitoring of total soil moisture on a scale of hectares using groundwater peizometers. *Geophysical Research Letters* **24**, 719–722 (1997).
36. Rasmussen, T. C. & Mote, T. L. Monitoring surface and subsurface water storage using confined aquifer water levels at the Savannah River Site, USA. *Vadose Zone Journal* **6**, 327–335, doi:10.2136/vzj2006.0049 (2007).
37. Marin, S., van der Kamp, G., Pietroniro, A., Davison, B. & Toth, B. Use of geological weighing lysimeters to calibrate a distributed hydrological model for the simulation of land-atmosphere moisture exchange. *Journal of Hydrology* **383**, 179–185 (2010).
38. Anochikwa, C. I., van der Kamp, G. & Barbour, S. L. Interpreting pore-water pressure changes induced by water table fluctuations and mechanical loading due to soil moisture changes. *Canadian Geotechnical Journal* **49**, 357–366 (2012).
39. Lambert, A. *et al.* Measuring water accumulation rates using GRACE data in areas experiencing glacialisostatic adjustment: The Nelson River basin. *Geophysical Research Letters* **40**, 6118–6122, doi:10.1002/2013GL057973 (2013).
40. McCutcheon, S. C., Martin, J. L. & Barnwell, T. O. In Handbook of Hydrology (ed. D. R. Maidment) 113 (McGraw-Hill, New York, 1993).
41. *R: A language and environment for statistical computing.* (The R Core Team, R Foundation for Statistical Computing, Vienna, Austria, 2013).
42. Bense, V. F. & Person, M. A. Transient hydrodynamics within intercratonic sedimentary basins during glacial cycles. *Journal of Geophysical Research:Earth Surface* (*2003-2012*) **113** (2008).

Acknowledgements

Author Contributions

W.G.B., R.G.T. and M.S. conceived the investigations and led the interpretation; A.Z. conceived preliminary investigations, and contributed experimental infrastructure and contextual data; R.G.T., M.S., A.Z., K.M.A. and D.J.L. installed the instrumentation; D.J.L. led the groundwater sampling and analysis; K.M.A. managed the data acquisition; M.S. led the data management; V.F.B. and W.G.B. designed the modelling scenarios; V.F.B. performed the modelling and contributed to the interpretation; W.G.B. drafted the manuscript; all authors reviewed the manuscript.

Additional Information

Supplementary information accompanies this paper at doi:10.1038/s41598-017-04159-w

Competing Interests: The authors declare that they have no competing interests.

Publisher's note: Springer Nature remains neutral with regard to jurisdictional claims in published maps and institutional affiliations.